Lung megakaryocytes are immune modulatory cells

Daphne N. Pariser, … , James Palis, Craig N. Morrell

Research Article Hematology Inflammation

Although platelets are the cellular mediators of thrombosis, they are also immune cells. Platelets interact both directly and indirectly with immune cells, impacting their activation and differentiation, as well as all phases of the immune response. Megakaryocytes (Mks) are the cell source of circulating platelets, and until recently Mks were typically only considered bone marrow–resident (BM-resident) cells. However, platelet-producing Mks also reside in the lung, and lung Mks express greater levels of immune molecules compared with BM Mks. We therefore sought to define the immune functions of lung Mks. Using single-cell RNA sequencing of BM and lung myeloid-enriched cells, we found that lung Mks, which we term Mk_L, had gene expression patterns that are similar to antigen-presenting cells. This was confirmed using imaging and conventional flow cytometry. The immune phenotype of Mks was plastic and driven by the tissue immune environment, as evidenced by BM Mks having an Mk_L-like phenotype under the influence of pathogen receptor challenge and lung-associated immune molecules, such as IL-33. Our in vitro and in vivo assays demonstrated that Mk_L internalized and processed both antigenic proteins and bacterial pathogens. Furthermore, Mk_L induced CD4^{+} T cell activation in an MHC II–dependent manner both in vitro and in vivo. These data indicated that Mk_L had key immune regulatory roles dictated in part by the tissue environment.

Find the latest version:

https://jci.me/137377/pdf

Lung megakaryocytes are immune modulatory cells

Daphne N. Pariser,[1,2] Zachary T. Hilt,[1] Sara K. Ture,[1] Sara K. Blick-Nitko,[1] Mark R. Looney,[3] Simon J. Cleary,[3] Estheany Roman-Pagan,[1] Jerry Saunders II,[4] Steve N. Georas,[2,5] Janelle Veazey,[2] Ferralita Madere,[2] Laura Tesoro Santos,[6] Allison Arne,[1] Nguyen P.T. Huynh,[7,8] Alison C. Livada,[1,9] Selena M. Guerrero-Martin,[10] Claire Lyons,[10] Kelly A. Metcalf-Pate,[10] Kathleen E. McGrath,[4] James Palis,[4] and Craig N. Morrell[1,2,5,9]

[1]Aab Cardiovascular Research Institute and [2]Department of Microbiology and Immunology, University of Rochester School of Medicine and Dentistry, Rochester, New York, USA. [3]Department of Medicine, UCSF, San Francisco, California, USA. [4]Center for Pediatric Biomedical Research, Department of Pediatrics, and [5]Department of Medicine, University of Rochester School of Medicine and Dentistry, Rochester, New York, USA. [6]Cardiovascular Research Department, University Hospital Ramón y Cajal Biotechnology, Medicine and Health Sciences PhD Program, University Francisco de Vitoria, Madrid, Spain. [7]Genomics Research Center, University of Rochester School of Medicine and Dentistry, Rochester, New York, USA. [8]Center for Translational Neuromedicine, University of Copenhagen, Copenhagen, Denmark. [9]Department of Pathology, University of Rochester School of Medicine and Dentistry, Rochester, New York, USA. [10]Department of Molecular and Comparative Pathobiology, The Johns Hopkins University School of Medicine, Baltimore, Maryland, USA.

Although platelets are the cellular mediators of thrombosis, they are also immune cells. Platelets interact both directly and indirectly with immune cells, impacting their activation and differentiation, as well as all phases of the immune response. Megakaryocytes (Mks) are the cell source of circulating platelets, and until recently Mks were typically only considered bone marrow–resident (BM-resident) cells. However, platelet-producing Mks also reside in the lung, and lung Mks express greater levels of immune molecules compared with BM Mks. We therefore sought to define the immune functions of lung Mks. Using single-cell RNA sequencing of BM and lung myeloid-enriched cells, we found that lung Mks, which we term Mk_L, had gene expression patterns that are similar to antigen-presenting cells. This was confirmed using imaging and conventional flow cytometry. The immune phenotype of Mks was plastic and driven by the tissue immune environment, as evidenced by BM Mks having an Mk_L-like phenotype under the influence of pathogen receptor challenge and lung-associated immune molecules, such as IL-33. Our in vitro and in vivo assays demonstrated that Mk_L internalized and processed both antigenic proteins and bacterial pathogens. Furthermore, Mk_L induced CD4+ T cell activation in an MHC II–dependent manner both in vitro and in vivo. These data indicated that Mk_L had key immune regulatory roles dictated in part by the tissue environment.

Introduction

Platelets are most commonly described as the megakaryocyte-derived (Mk-derived) cellular mediators of thrombosis. Mk differentiation and platelet production have been extensively studied in the bone marrow (BM) environment, but recent research has expanded our prior limited view of both platelet origins and platelet functions. Platelets are increasingly appreciated as having diverse inflammatory and immune regulatory roles (1), and despite studies going back to 1893 demonstrating that Mks reside in the lungs, lung Mks were only recently shown to be a significant source of circulating platelets (2–6). These novel emerging concepts of platelet functions and origins are rapidly reshaping how we view platelets in both health and disease.

Activated platelets either express or secrete abundant inflammatory and immune molecules that recruit and activate leukocytes, both at sites of platelet deposition and systemically (7–12). Platelets and platelet-derived immune mediators contribute to the initiation or acceleration of inflammatory diseases such as atherosclerosis and asthma, as well as responses to bac-

terial and viral infection (13–15). The large number of circulating platelets and the diversity of their inflammatory molecules, including platelet factor 4 (PF4), CCL5, CD154, β2M, and transforming growth factor beta (TGF-β), give platelets important and diverse immune functions relevant in many disease contexts (2, 11, 16–18). We have shown that platelets initiate, accelerate, and regulate all phases of the immune responses, including platelet induction of an acute-phase response (19), regulation of monocyte trafficking and differentiation (17), induction and maintenance of T helper cell differentiation (20), and platelet processing and presentation of antigen to CD8+ T cells (21). Others have demonstrated that Mks can cross present antigen in vitro (22). These studies demonstrate a central role for platelets and Mks in both innate and acquired immune responses. More recent studies demonstrated that intravascular lung Mks produce circulating platelets and identified non–platelet-producing, sessile Mks in lung interstitial tissue (2). Bulk RNA sequencing (RNA-seq) data compared BM and lung Mks and showed that lung Mks were enriched with mRNAs associated with immune regulatory functions, including mRNAs for many immunoreceptors, chemokines, and cytokines (2). The role of Mks as immune regulatory cells is poorly understood in general, but particularly so with lung Mks. Lung Mks increase in number during pulmonary and cardiovascular diseases, further suggesting they may be dynamic and responsive to inflammatory states (23).
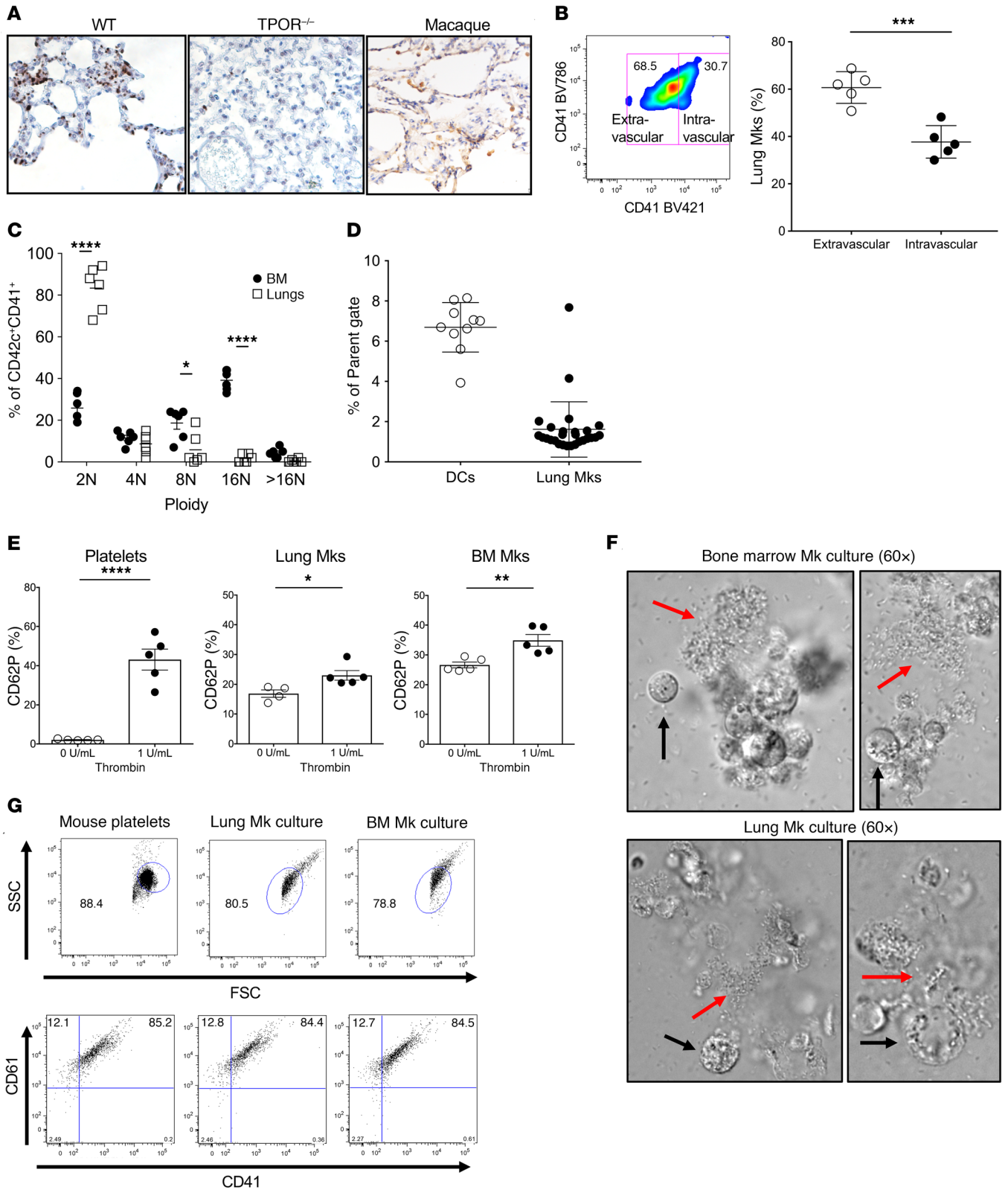
Figure 1. Lung and BM Mks are phenotypically distinct. (A) Mks are present in the lung. Lung sections from WT mice, TPOR$^{-/-}$ mice, and macaques were immunostained with anti-CD42c antibody (mouse tissue) or anti-CD41 (macaque). Mks were noted in WT mouse and primate lungs (representative images). Original magnification, ×40. **(B)** Mks are both intravascular and extravascular in the lung. Tissue and vascular discrimination between the lung Mks using anti-CD41 BV421 and BV786 by flow cytometry (unpaired t test). **(C)** BM Mk ploidy is greater than that of lung Mks. BM and lung Mk ploidy determined by flow cytometry (2-way ANOVA with Šidák's multiple-comparison test). **(D)** The percentage of Mks relative to DCs in digested and single-cell resuspended lung tissue. Approximately 2% are Mks compared with 7% resident lung DCs (CD103$^+$CD11b$^+$). **(E)** Lung and BM Mks upregulate P-selectin (CD62P) in response to thrombin. Isolated lung and BM Mks were stimulated with 1 U/mL thrombin and CD62P surface expression determined by flow cytometry as a marker of degranulation (unpaired t test). **(F)** Lung Mks produce platelets in vitro. FRET imaging was used to obtain images of proplatelet production from both BM and lung Mks in culture. The red arrows indicate proplatelet formation, while the black arrows indicate an Mk. **(G)** Flow cytometry confirmation of platelet production in the Mk cultures. Freshly isolated mouse platelets were used as a control. $*P = 0.01$ to 0.05; $**P = 0.001$ to 0.01; $***P = 0.0001$ to 0.001; $****P < 0.0001$.

Lungs and BM are very different tissue environments. Compared with the lung, the BM faces few pathogen challenges, is relatively hypoxic, and is an immune suppressive environment. In contrast, the lung has a microbiome, high O_2, and the lung tissue environment is primed to induce immune cell activation (24–26). Cells in the lung, such as airway epithelial cells, produce cytokines in response to pathogens or immune challenges that regulate immune cell differentiation, including the maturation of lung dendritic cells (DCs) (27). Mks come from hematopoietic stem cells (HSCs) and develop under the influence of thrombopoietin (TPO). Because Mks have only been studied in the immune-quiescent BM environment, it is not known whether Mks in other tissues have a different immune phenotype and functions. Our data demonstrate that lung and BM Mks have distinct immune phenotypes and functions; lung Mks secrete inflammatory cytokines and express molecules that are similar to many tissue-resident leukocytes and antigen-presenting cells (APCs), and lung Mks process live intact bacteria and present bacteria-derived antigen to CD4$^+$ T cells both in vitro and in vivo. Our in vivo data suggest that lung Mks have important roles in the early activation of T cell responses to a pulmonary pathogen challenge, identifying what we believe is a novel immune regulatory role for lung Mks.

Results

To verify the presence of Mks in the lung, immunohistochemistry with anti-CD42c antibody was performed on lung tissue isolated from WT and Mk-deficient TPO receptor–knockout (TPOR$^{-/-}$) (28) mice as a negative control. To demonstrate the presence of lung Mks in primates, macaque monkey lungs were also immunostained with anti-CD41 antibody. Mks were diffusely distributed throughout both stained WT mouse and primate lungs (Figure 1A). To determine the intravascular versus extravascular (interstitial) distribution of lung Mks, mice were injected i.v. with a BV421-labeled anti-CD41 antibody and 3 minutes later mice were sacrificed and subsequently isolated lung cells were stained with an anti-CD41 antibody with a different fluorescent label (BV786)

(29). Similar to published reports (2), approximately 60% of lung Mks were extravascular (Figure 1B). Because lung Mks appear smaller than BM Mks in tissue sections, we determined their ploidy and found that lung Mks were primarily 2N (Figure 1C), potentially explaining why their presence in the lung has been largely overlooked, as studies have noted that lung Mks are present at a density of approximately 18 Mks/cm^2 of lung tissue and make up about 8% of total Mks in the body (23, 30). Using collagenase-digested lungs and flow cytometry we next assessed the number of lung Mks relative to DCs as an immune cell comparison. Mks were approximately 2%–3% of the cells isolated following collagenase digestion, versus lung DCs (CD103$^+$CD11b$^+$), which were approximately 6%–7% of the cells (Figure 1D).

To facilitate lung Mk characterization, we used a negative-selection protocol; the purity of the Mk isolation was confirmed by imaging flow cytometry (Supplemental Figure 1; supplemental material available online with this article; https://doi.org/10.1172/JCI137377DS1). We also confirmed that isolated lung Mks maintain a mature Mk phenotype in cell culture (Supplemental Figure 2). To demonstrate that lung Mks have typical Mk characteristics, isolated platelets, BM Mks, and lung Mks were stimulated with thrombin. BM Mks and lung Mks similarly upregulated CD62P in response to thrombin (Figure 1E). After 4 days in culture, platelet generation from BM and lung Mks was also assessed by microscopy and flow cytometry (Figure 1, F and G). Lung and BM Mks each produced platelets in vitro.

Bulk RNA-seq of isolated lung and BM Mks indicated that lung Mks had an immune-differentiated phenotype relative to BM Mks. To gain a deeper analysis of gene expression differences between BM and lung Mks in relation to myeloid cells in each tissue, we performed single-cell RNA-seq (scRNA-seq) and integrated cluster analysis on myeloid cell– and Mk-enriched BM and lung cell isolates (other cell lineages were depleted by positive selection). Mks identified by analysis of enriched Mk gene markers (*Pf4*, *Itga2b*, *Ppbp*, *Itgb3*, *Gp9*, and *Cxcr4*; Supplemental Table 1) clustered as genetically distinct populations, while lung Mks clustered closely with both BM and lung DCs (Figure 2A). Further gene expression analysis indicated that lung Mks expressed numerous immune-related genes, including many commonly associated with DCs (Figure 2A and Supplemental Figures 3–5). These data were validated in part using imaging flow cytometry to rule out the potential for analyzing myeloid cells with adherent platelets. Lung Mks, but not BM Mks, expressed MHC II and DC markers such as CD11c (Figure 2B and Supplemental Figure 6). Mks were further phenotyped for APC-like markers including MHC II, CD80, CD40, ICAM-1, LFA-1, and CCR7 (Figure 2C and Supplemental Figure 7), which were all expressed at high levels on lung Mks relative to BM Mks. Additionally, macaque lung Mks had an APC-like immune phenotype similar to that of mouse lung Mks (Figure 2D and Supplemental Figure 8). Taken together, these data indicate that unlike BM Mks, lung Mks, which we now term Mk$_L$ to emphasize their unique immune molecule expression relative to BM Mks, have an immune phenotype with several characteristics typical of an APC.

Lungs and BM are very different tissue environments; BM is sterile and hypoxic, while lungs face constant pathogen/antigen challenges and high O_2 exposure. Newborn postnatal day 0 (P0) mouse lungs have not had prolonged O_2 exposure or antigen chal-
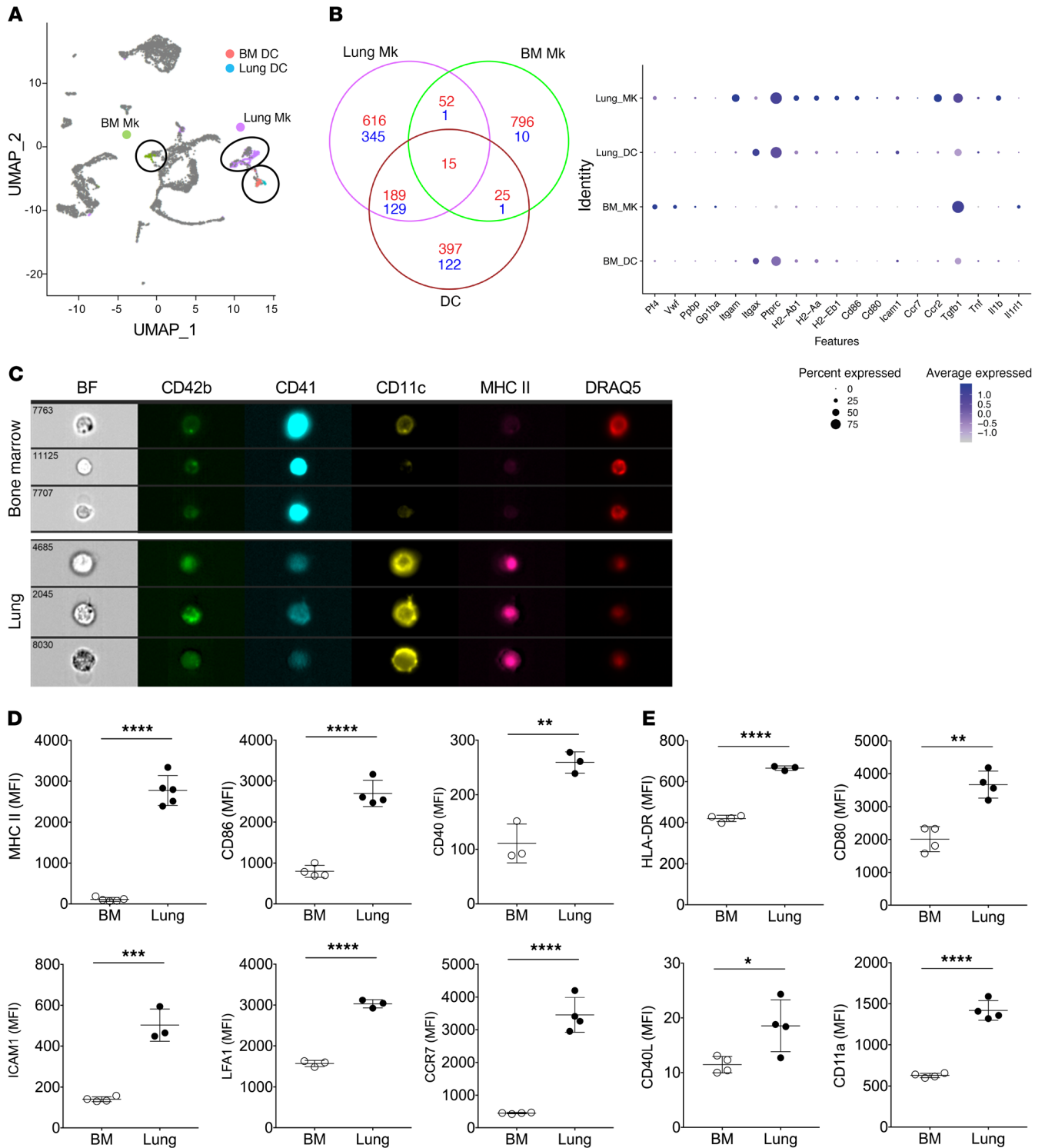
Figure 2. Lung and Mk immune molecule expression. (**A**) Integration of BM and lung scRNA-seq data. BM and lung Mks had distinct mRNA expression. (**B**) Venn diagram and dot plot from scRNA-seq. Wilcoxon's rank sum test (Seurat FindMarkers function) was performed and genes differentially expressed in the clusters of interest (Mks or DCs) against all other clusters were identified (adjusted P value < 1 × 10^{-3}). Positive markers in red, and negative markers in blue. Dot plot indicates the average expression and proportion of cells expressing genes of interest. (**C**) Mk characterization using imaging flow cytometry. Lung Mks expressed more CD11c and MHC II compared with BM Mks. BF, bright field. (**D**) Comparison of mouse lung and BM Mk APC-related molecule expression by flow cytometry. Lung Mks express more APC-associated molecules (unpaired t test). (**E**) Comparison of primate lung and BM APC-related molecule expression. Lung Mks expressed more APC-associated molecules (unpaired t test). *P = 0.01 to 0.05, **P = 0.001 to 0.01, ***P = 0.0001 to 0.001, ****P < 0.0001.
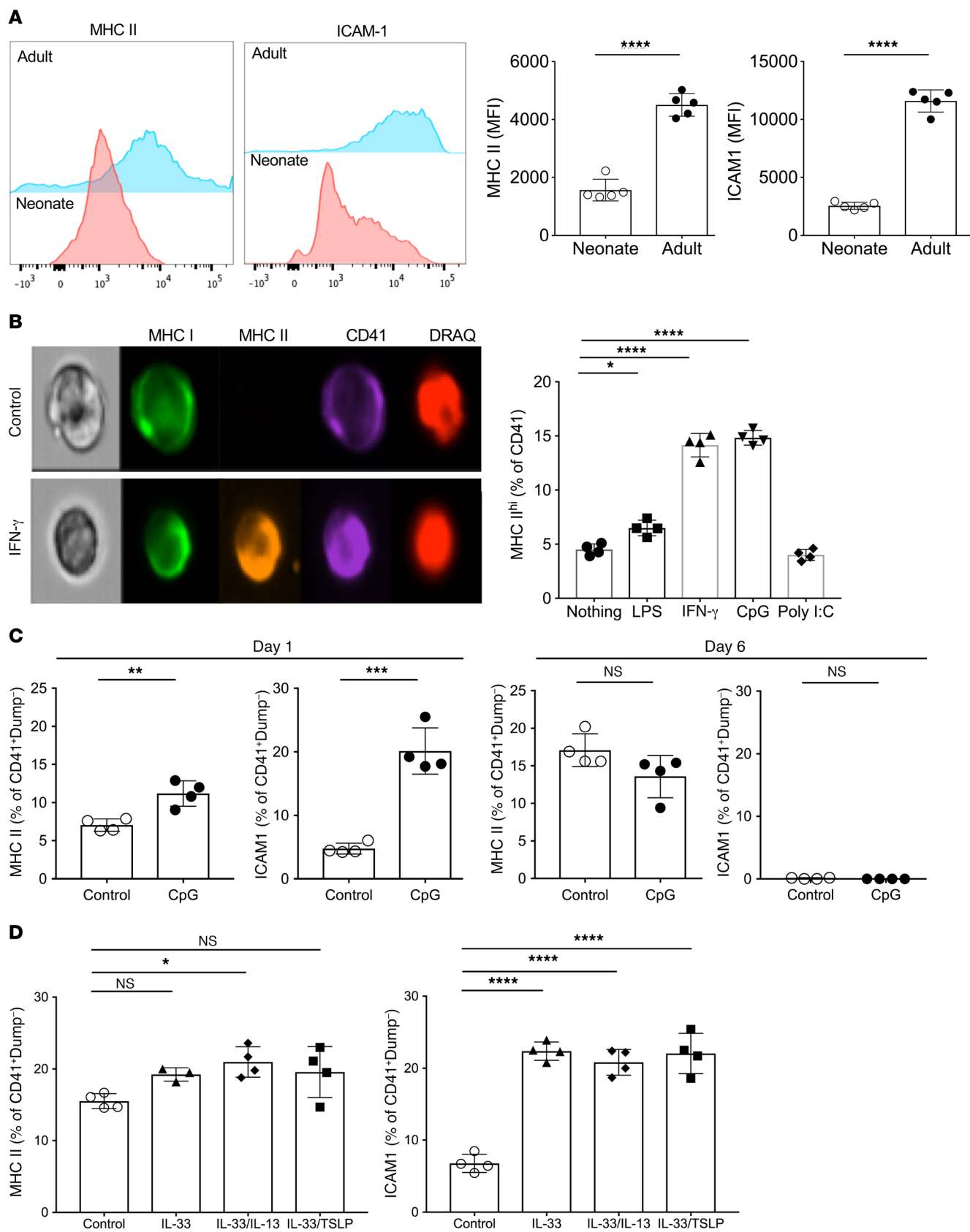
Figure 3. Lung Mk immune phenotype is environmentally regulated. (A) MHC II and ICAM1 expression on Mks from P0 and adult mice. Neonatal lung Mks had reduced MHC II and ICAM1 compared with adult lung Mks (unpaired t test). **(B)** BM Mks increased MHC II expression in response to immune stimuli. BM Mks were incubated with immune stimuli for 48 hours and MHC II expression determined. LPS, INF-γ, and CpG increased MHC II (1-way ANOVA with Tukey's multiple-comparison test). **(C)** BM Mks respond to CpG within 24 hours and the expression of immune molecules is similar to that of control BM Mks at day 6 (unpaired t test). **(D)** Lung-derived immune modulatory cytokines induced BM Mk immune differentiation. BM Mks were incubated with IL-33 or IL-33 in combination with other common lung cytokines. Forty-eight hours later immune differentiation was determined (1-way ANOVA with Tukey's multiple-comparison test). *P = 0.01 to 0.05; **P = 0.001 to 0.01; ***P = 0.0001 to 0.001; ****P < 0.0001.

lenges, and P0 lungs have an immature immune cell population (25). To begin to determine whether the tissue environment influences Mk_L differentiation, we compared P0 neonatal and adult mouse lung Mks. MHC II and ICAM1 were each expressed at much higher levels on adult compared with P0 mouse Mk_L, suggesting that the Mk immune phenotype may be regulated by the postnatal environment (Figure 3A). To explore a potential role for O_2 in Mk_L immune differentiation, isolated BM Mks were exposed to hypoxic or normoxic (5% or 21% O_2) conditions in vitro for 48 hours. MHC II expression was not changed by incubation in hypoxic conditions, indicating that O_2 is unlikely to regulate Mk immune differentiation (Supplemental Figure 9). To investigate whether Mks have immune plasticity, BM Mks were incubated in vitro with pathogen-associated and/or cytokine-mediated stimulation. Isolated BM Mks were stimulated with the pathogen receptor agonists LPS (TLR4 agonist), CpG (TLR9 agonist), poly(I:C) (TLR3 agonist), or with interferon gamma (IFN-γ). We found that LPS, CpG, and IFN-γ increased BM Mk MHC II expression, but poly(I:C) (TLR3 agonist) did not (Figure 3B and Supplemental Figure 10). To determine whether this immune activation was long lived or had plasticity, BM Mks were stimulated with CpG and MHC II and ICAM1 expression determined 1 and 6 days later. By day 6 control and CpG-treated Mk MHC II was similarly expressed, and ICAM1 expression was undetectable in either condition (Figure 3C). These data further indicate that Mks are similar to other immune cells in their immune plasticity.

The cell composition and cytokine milieu greatly differs between lungs and BM. Tissue-resident cells in the lung, such as airway epithelial cells, secrete cytokines that promote DC maturation, including IL-33, IL-13, and TSLP, whereas the BM is immune suppressive (31). IL-33, either alone or with the other lung DC maturation cytokines, increased BM Mk MHC II and ICAM1 expression (Figure 3D). To explore whether IL-33 in part regulates Mk_L immune differentiation in vivo, mice were treated with anti-CD42b antibody (or control IgG) to deplete platelets and Mk_L, but not BM Mks (Supplemental Figures 11 and 12). Twenty-four hours later mice were treated with ST2/IL-33R-Fc chimeric protein (ST2-Fc) to block IL-33 during Mk_L recovery. On day 4 after recovery, Mk_L expressed higher levels of MHC II compared with control mouse Mk_L (Figure 4A). However, blocking IL-33 reduced MHC II expression on recovering Mk_L (Figure 4A). To further demonstrate a potential role for IL-33 in Mk_L immune differentiation, neonatal mice were treated with control IgG or ST2-Fc on P1 and P4, and

Mk_L immune phenotype determined on day P7. Blocking IL-33 reduced Mk_L MHC II and ICAM1 (Figure 4B). Taken together, these data suggest a role for IL-33 in Mk_L immune differentiation.

To further demonstrate a role for the lung environment in Mk immune differentiation, BM Mks were isolated, fluorescently labeled, and then delivered via the oropharyngeal (o.p.) route to recipient mice (control mice given buffer only). Two days later transferred cells were recovered and assessed by flow cytometry. Transferred BM Mks acquired an Mk_L-like immune phenotype in the lung, including increased MHC II and CCR7 (Figure 4C), indicating that the lung environment may dictate Mk immune differentiation. We also found on day 5 that some lung-transferred BM Mks migrated to the BM, but these migrated Mks expressed less MHC II and CCR7 compared with the Mks that remained lung resident (Figure 4D). Together, these data demonstrate that the Mk phenotype is also plastic in vivo and altered by the tissue environment.

We next asked whether primary Mk_L and BM Mks differ in their responses to immune stimuli. To begin to address this question, we isolated Mk_L and BM Mks, and Mks were stimulated overnight with LPS (10 ng/mL) or control buffer. As a control, BM-derived DCs (BMDCs) were prepared and also treated with buffer or LPS. The supernatants were analyzed by cytokine membrane array. Compared with BM Mks, Mk_L secreted more immune molecules that were similar to the molecules secreted by LPS-challenged BMDCs (Figure 5, A and B). These data were confirmed by measuring KC secretion, which was found to be much higher in the supernatant of LPS-stimulated Mk_L than BM Mks (Figure 5C).

For a cell to function as an APC it must internalize and process an antigen to present it to CD4+ T cells. To determine whether Mks process antigen, we cultured primary BM Mks and Mk_L with DQ-ovalbumin (DQ-Ova, 200 μg/mL) and cell fluorescence was determined by flow cytometry 30 minutes later as a measure of Ova processing (DQ-Ova is only fluorescent following cleavage). BM Mks and Mk_L similarly processed Ova antigen in vitro (Figure 5D). To determine whether Mk_L acquire and process antigen in vivo, PF4 reporter mice (Pf4^Cre-Rosa26-LSL-tdTomato mice) were challenged with LPS (0.5 mg/kg) and then DQ-Ova was delivered via the o.p. route. The lungs were then live imaged for 80 minutes. PF4+ cells acquired and processed DQ-Ova (Figure 6A). DQ-Ova was also noted in Mk_L 24 hours after o.p. delivery (Figure 6B). To compare the ability of Mk_L and BM Mks to take up bacteria, isolated Mks were cocultured with live GFP+ $E.$ $coli$ for 30 minutes and imaging flow cytometry was used to measure intracellular bacteria. Although Mk_L and BM Mks both phagocytosed $E.$ $coli$, Mk_L internalized more $E.$ $coli$ (Figure 6C [representative images], Figure 6D [quantification], and Supplemental Figure 13). To confirm Mk phagocytosis, we utilized PhrodoGreen bacteria, which are only fluorescent when internalized into a phagolysosome and digested. PhrodoGreen bacteria were incubated with isolated BM Mks, Mk_L, or a macrophage cell line, RAW cells. Mk_L phagocytosed more PhrodoGreen bacteria compared with BM Mks, which was limited by cold incubation (Supplemental Figure 14). GFP+ $E.$ $coli$ were also delivered to mice via the o.p. route and 3 hours later the number of GFP+ Mk_L and DCs was similar (Figure 6E). These data demonstrate that Mk_L are phagocytic and can acquire inhaled antigens and pathogens.
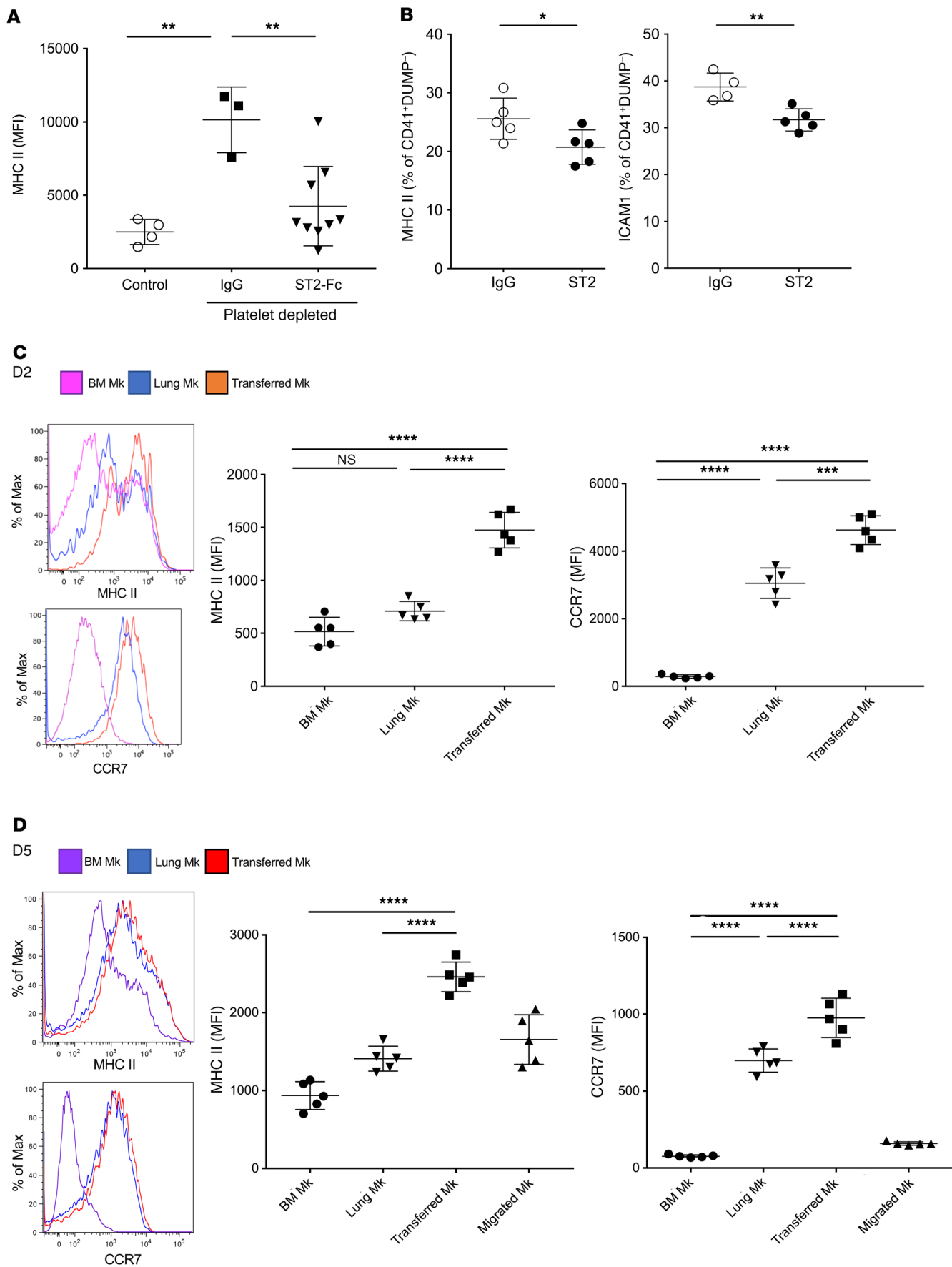
Figure 4. In vivo regulators of lung Mk phenotype. (A) IL-33 promoted lung Mk immune differentiation in vivo. Mice were treated with Mk-depleting antibody or control IgG. Mice were then treated with either ST2-Fc as an IL-33 blocking agent or control IgG. Recovering Mks had increased MHC II that was greatly attenuated by IL-33 blocking (unpaired t test). **(B)** P0 mice were treated with IgG or ST2-Fc and on P7 the lung Mk immune phenotype determined. IL-33 blocking reduced postnatal lung Mk immune differentiation (unpaired t test). **(C** and **D)** BM Mk immune phenotype plasticity in vivo. BM Mks were isolated, labeled with CFSE, and o.p. delivered to control mice. **(C)** Two days and **(D)** 5 days later transferred BM Mk MHC II and CCR7 levels were determined. BM-transferred BM Mks had increased immune molecule expression in the lung environment. After 5 days **(D)**, BM Mk cells transferred to the lung were also identified in the BM and had reduced immune molecule expression compared with those transferred and in the lung (1-way ANOVA with Tukey's multiple-comparison test). *P = 0.01 to 0.05; **P = 0.001 to 0.01; ***P = 0.0001 to 0.001; ****P < 0.0001.

Because Mk_L cells expressed MHC II and acquired antigen, we next asked whether Mk_L can present antigen to CD4$^+$ T cells in vitro. Isolated Mk_L and BMDCs were stimulated with LPS, incubated with Ova, and cocultured with OTII T cells that recognize Ova presented in the context of MHC II for 3 days. Mk_L activated OTII T cells in an Ova-dependent manner, and to a much greater extent than did BM Mks (Figure 7A). To begin to determine whether Mk_L present antigen in vivo, OTII T cells were transferred to WT or TPOR$^{-/-}$ mice (TPOR$^{-/-}$ mice have greatly reduced numbers of Mks and circulating platelets; ref. 28). Twenty-four hours after OTII cells were infused, mice were given Ova-expressing *E. coli* (*E. coli*^{OVA}) via the o.p. route. OTII cell activation in the lungs and mediastinal lymph nodes (mLNs) was then determined on day 3 by flow cytometry. Infected WT and TPOR$^{-/-}$ mice had similar post-infection weight loss, indicating similar infections (Supplemental Figure 15); however, OTII T cells in the lungs and mLNs of WT infected mice were more activated compared with those in TPOR$^{-/-}$ mice (Figure 7B and Supplemental Figure 16). These data indicate that Mk_L may regulate CD4$^+$ T cell responses to lung infection.

Because the TPOR$^{-/-}$ mice also have greatly reduced platelet counts, we could not rule out a platelet-mediated OTII response mechanism. Therefore, we next asked whether Mk_L can directly present antigen to CD4$^+$ T cells in an MHC II–dependent manner. Mk_L were isolated from WT and MHC II$^{-/-}$ mice and cocultured with OTII T cells and Ova. Naive OTII T cell activation was assessed 3 days later and found to be greatly reduced with MHC II$^{-/-}$ Mk_L coincubation (Figure 7C). In a separate experiment, OTII T cells were cocultured with WT Mk_L, MHC II$^{-/-}$ Mk_L, or BMDCs and Ova for 8 days and IL-2 production determined by ELISA. IL-2 increased in WT, but not MHC II$^{-/-}$ Mk_L and BMDC cocultures (Figure 7D). These data indicate that Mk_L activate CD4$^+$ T cells in an MHC II–dependent manner.

To more specifically determine whether Mk_L-mediated lung CD4$^+$ T cell responses are MHC II dependent, we made Pf4^{Cre}-MHC II$^{fl/fl}$ (Mk-MHC II$^{-/-}$) mice. WT and Mk-MHC II$^{-/-}$ mice had similar immune cell development and platelet activation (Supplemental Figures 17–21), and Mk_L, but not DCs, had reduced MHC II expression (Supplemental Figure 22). WT and Mk-MHC II$^{-/-}$ mice each received OTII T cell transfer and *E. coli*^{OVA} infection (Supplemental Figure 23). On day 3 after infection, OTII T cells in WT mouse lungs had increased CD25 and more prolifer-

ation compared with Mk-MHC II$^{-/-}$ mice (Figure 7E). OTII T cells in mLNs were similar in both WT and Mk-MHC II$^{-/-}$ mice (Supplemental Figure 24), demonstrating that CD4$^+$ T cell activation in the lung is at least in part Mk MHC II dependent. Endogenous T cells showed no activation, indicating antigen specificity (Supplemental Figure 25).

Discussion

Taken together, these data support the concept that Mk_L and BM Mks share many Mk-specific characteristics, such as common cell markers and the ability to produce platelets (2), but Mk_L also have immune cell characteristics that differ from BM Mks. Furthermore, these location-specific cell characteristics may in part be driven by the tissue environment. Immune molecule expression and immune characteristics of Mk_L include their having in vitro and in vivo APC-like cell markers and functions. Our scRNA-seq data, validated by flow cytometry, indicated that Mk_L expressed a number of genes in common with both BM Mks and DCs. We also demonstrated that the Mk_L immune phenotype is at least in part shaped by their tissue environment, as the lung is continuously exposed to pathogens and lung cells secrete cytokines, such as IL-33, which contribute to Mk_L immune differentiation. In contrast, the BM is an immune suppressive tissue environment. We demonstrated the differential ability of Mk_L to mediate host responses to pathogenic challenges in vitro and in vivo, suggesting that Mk_L and BM Mks have distinct immune functions, and that Mk_L may have roles in pulmonary immune responses. With further investigation, these finding may impact our understanding of many common pulmonary diseases such as asthma and allergy, lung infections, and pulmonary hypertension, providing potential new avenues for therapeutic development.

Although interest in and study of lung Mks has recently increased, Mks were long ago described in human lungs, liver, spleen, peripheral blood, and umbilical cord blood (6). As long ago as 1948, intrapulmonary Mks were found to be present across 30 human necropsies, and were described as having a density of 14–65 Mks/cm^2 in lung sections (32), with the highest concentration of Mks being found in the central zone of the right upper lobe of the lung (23). As early as 1937, platelet production was proposed to occur in the lung (33), and this was recently more definitively demonstrated by Lefrançais et al. (2). The developmental origins of lung Mks is not yet clear. A common notion that is lacking experimental evidence is that lung Mks are derived from the BM and become trapped in the small vessels of the lung. Both our data and prior data demonstrate that there is an intravascular and a substantial interstitial population of lung Mks (2). This implies that if Mk_L are BM derived when they reach the lung, they must migrate out of the vasculature and into the lung tissue. Lungs do have HSCs and lung-derived HSCs can repopulate the BM and vice versa (2). Most of the knowledge we currently have about HSC niches and hematopoietic cell development is based on data from BM-focused studies, as it is clearly the major site of hematopoietic cell development. However, given the presence of HSCs in the lung, the presence of extravascular lung Mks, and the unique phenotype of Mk_L, more work is needed to definitively determine the origin and differentiation of Mk_L.
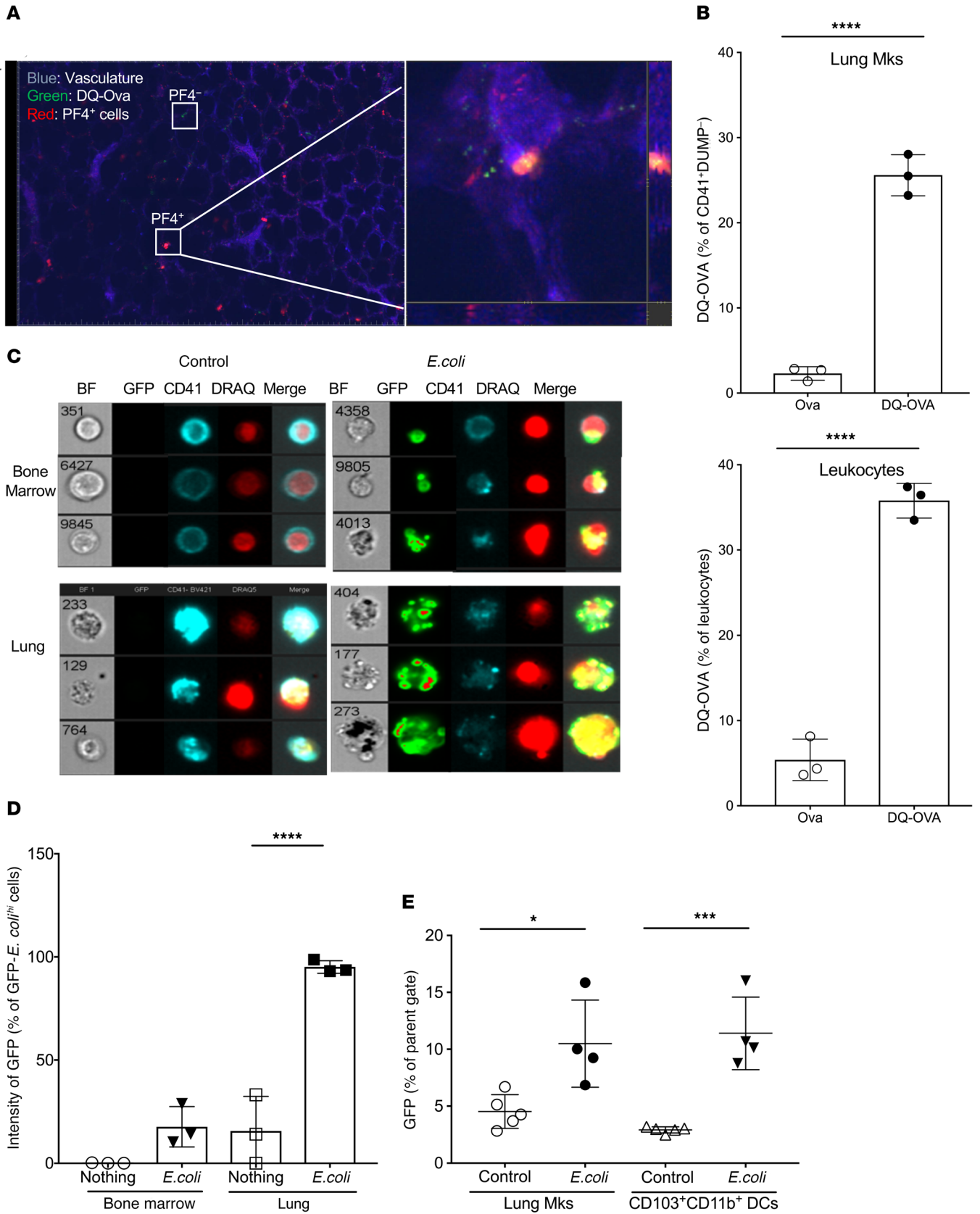
Figure 5. Lung Mks process and present antigen. (A and B) Lung Mks had greater LPS-induced inflammatory molecule production compared with BM Mks. Mks were incubated for 24 hours with control buffer or LPS. Inflammatory molecules were identified by a (A) cytokine array and (B) relative intensities compared with control plotted as a heatmap. (C) KC in the supernatant measured by ELISA. (D) Antigen processing in vitro. Mks were incubated with DQ-Ova for 30 minutes and fluorescence was determined by flow cytometry (unpaired t test). ***P = 0.0001 to 0.001, ****P < 0.0001.

Immune cells, such as macrophages, are typically classified by their cell surface markers, and then subtyped by both their differentiation-associated markers and their functional phenotype in a tissue environment. Our data argue that Mks may also follow this paradigm. Mks in both the lung and BM express a core set of cell markers and have a common set of cell functions, including the ability to produce platelets. However, similar to macrophages, our results indicate that Mks also exhibit tissue- and inflammatory environment–dependent immune plasticity. We have therefore chosen to refer to lung Mks as Mk$_L$ to emphasize the tissue-

Figure 6. Lung Mks process and present antigen in vivo. (**A**) Mice were treated with control buffer or DQ-Ova via the o.p. route. Eighty minutes later real-time in vivo lung imaging was performed (representative image). (**B**) Twenty-four hours later DQ-Ova lungs were also isolated to quantify fluorescent Mks. Lung Mks internalized antigen (unpaired *t* test). (**C** and **D**) Lung Mks are more phagocytic than BM Mks. BM and lung Mks were incubated with control buffer or GFP *E. coli* and 30 minutes later fluorescence was determined by (**C**) ImageStream (representative images) and (**D**) bacteria internalization was quantified (unpaired *t* test). BF, bright field. (**E**) Lung Mks take up *E. coli* in vivo. *E. coli* was delivered via the o.p. route and 3 hours later *E. coli*–positive lung Mks and DCs were quantified by flow cytometry (unpaired *t* test). *P = 0.01 to 0.05; ***P = 0.0001 to 0.001; ****P < 0.0001.

dependent immune phenotype. As noted above, it is still unclear whether, similar to tissue-resident macrophages, a population of Mk_L may proliferate locally in the lung. It also remains to be determined whether the immune and platelet production phenotype of interstitial and intravascular Mk_L differs and whether the Mk_L and BM Mk populations are derived from the same precursors. We cannot definitively rule out that Mk_L are a myeloid lineage cell that in the lung tissue has gene and protein markers in common with Mks, as the definitive origin of Mk_L is still not known. Research tools remain to be developed to address these remaining questions of Mk_L origin that may shape their functions.

Results of the studies in this work may also lead to a better understanding of the pathogenesis of lung diseases ranging from infectious pneumonias, to asthma, and pulmonary hypertension. Although DCs clearly have a major role in CD4+ T cell responses, therapies solely aimed at DCs may be missing other relevant immune cells in the lung, including Mk_L, as our data indicate that a reduction in Mk MHC II in the lung results in decreased lung CD4+ T cell activation in an antigen-specific manner. TPOR$^{-/-}$ mice deficient in Mks and platelets had only limited CD4+ T cell activation. This implies that Mk_L or circulating platelets support CD4+ T cell responses to lung pathogens by mechanisms beyond directly presenting antigen. This likely includes the secretion of Mk_L cytokines or chemokines that help to drive immune responses and development beyond direct antigen presentation. Although we have focused on this intriguing T cell activating function for lung Mk_L, they are likely to have important roles in all phases of lung immune responses. Mk_L may also be important in immune homeostasis, as we have shown that platelets maintain both basal T helper cell and monocyte immune phenotypes. Mk_L may therefore have key roles in lung immune quiescence in healthy conditions that remain to be discerned.

These studies demonstrate an important immune function for Mks in the lung and represent a potentially novel concept — Mk_L can internalize, process, and present antigen to CD4+ T cells. While more work needs to be done to determine the disease relevance of these studies and the ontogeny of Mk_L, these data lay the foundation for better understanding Mk_L functions and origins.

Methods

Mice. All mice used in our studies were on a C57BL/6J background. Mice that were not bred in house were purchased from Jackson Labs. All mice used were 8 to 12 weeks of age and a mix of males and females in our in vivo experiments. I-AB–floxed mice (MHC II$^{-/-}$; stock number 003584) and Pf4-Cre mice were purchased from Jackson Labs. TPOR$^{-/-}$ mice were used in prior studies by our laboratory (17, 20).

Single-cell suspension for cell culture, ImageStream flow cytometry, flow cytometry, and scRNA-seq. Whole lungs were removed and put into complete DMEM with 1 mg/mL collagenase type II (Thermo Fisher Scientific, NC9693955). Complete DMEM consisted of 10% FBS (Invitrogen), penicillin/streptomycin (Invitrogen, 15-140-122), vitamins (Invitrogen, 11120052), Glutamax (Invitrogen, 10566016), nonessential amino acids (Invitrogen, 11140050), and sodium pyruvate (Invitrogen, 11-360-070). Lungs were incubated at 37°C for 30 minutes and then mashed through a 100-μm cell strainer (Thermo Fisher Scientific, 08-771-19). ACK Lysing Buffer (Thermo Fisher Scientific, A1049201) was added to the single-cell suspension and this mixture was spun down at 135g for 5 minutes. The ACK was washed out with 50 mL of isolation buffer, which consisted of 1 mM EDTA and 2.5% FBS in PBS.

For Mk isolation, a negative-selection protocol was used that included biotinylated anti-CD11b (BioLegend, NC0200884), -B220 (BioLegend, NC0200885), -CD3ε (BioLegend, 100304), and -CD146 (BioLegend, 134716) antibodies and incubating in a 5 mL polystyrene tube (Laboratory Product Sales, L285601) with 50 μL/mL of rat serum. All antibodies were at 5 μg/mL final concentration and streptavidin beads (STEMCELL Technologies, 19860) at 75 μL/mL of sample (under 1×10^9 cells) concentration added. Each sample was then added to a magnet and incubated for 3–5 minutes and non-bound cells transferred to a 15 mL tube with prewarmed complete DMEM.

Cells from tibias and femurs were isolated by flushing the BM with isolation buffer using a 20-gauge needle (BD Biosciences, 14-826D). If Mks were used for experimentation, the same procedure that was used for the lungs was used for the BM. For BMDCs we followed the protocol provided by Abcam (https://www.abcam.com/protocols/bmdc-isolation-protocol).

Flow cytometry and ImageStream reagents. Antibodies against the following proteins were used: CD41 (MWReg30, BioLegend), MHC II (M5/114.15.2, BioLegend), CD54 (YN1/1.7.4, BioLegend), CD69 (H1.2F3, BioLegend), CD4 (GK1.5, BioLegend), CD205 (NLDC-145, BioLegend), CD207 (4C7, BioLegend), CD8α (53-6.7, BioLegend), CD326 (G8.8, BioLegend), CD103 (2E7, BioLegend), CD105 (SN6h, BioLegend), CD252 (RM134L, BioLegend), Ly-6C (HK1.4, BioLegend), CD62P (RMP-1, BioLegend), CD3 (17A2, BioLegend), CD86 (GL-1, BioLegend), CD19 (MB19-1, BD Biosciences), CD19 (1D3/CD19, BioLegend), CCR7 (4B12, BioLegend), CD25 (3C7, BioLegend), CD11b (M1/70, BioLegend), TER-119 (TER-119, BioLegend), H-2Db (KH95, BioLegend), CD45 (PI62251, BioLegend), and IFN-γ (XMG1.2, BioLegend). The following reagents were also used: Leukocyte Activation Cocktail, with BD GolgiPlug (Thermo Fisher Scientific, BDB550583), Cell Activation Cocktail (without brefeldin A) (BioLegend, 50-712-273), Brilliant Stain Buffer (BD Biosciences, BDB563794), OneComp eBeads (Thermo Fisher Scientific, 50-112-9031), Corning Falcon Round-Bottom Polystyrene Tubes (Corning, 352054), and DRAQ5 Fluorescent Probe Solution (Thermo Fisher Scientific, PI62251).

scRNA-seq. Cell suspensions were loaded on a Chromium Single-Cell Instrument (10× Genomics) to generate single-cell gel bead-in-emulsions (GEMs). Libraries were prepared using a Chromium Single-Cell 3′ Library & Gel Bead Kit (10× Genomics). The beads were dissolved and cells were lysed per manufacturer's recommendations. GEM reverse transcription (GEM-RT) was performed to produce
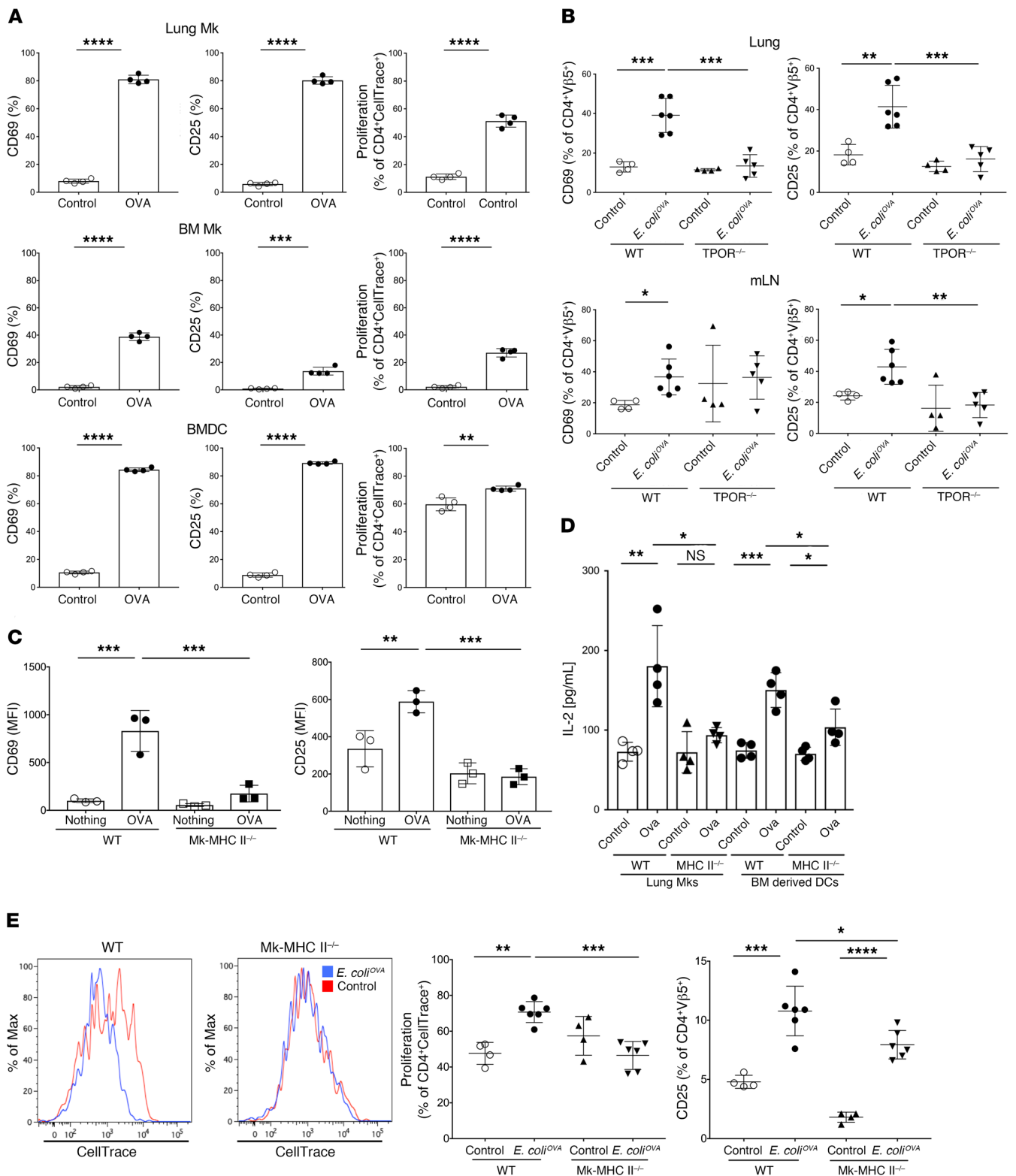
Figure 7. Lung Mks present antigen. (**A**) Lung Mks activated OTII T cells in vitro. T cells were cocultured with lung Mks or splenocytes and on day 3 T cell activation was determined (unpaired *t* test). (**B**) Mice lacking Mks had reduced antigen-specific T cell responses in vivo. WT and TPOR^{–/–} mice were given OTII T cells and 24 hours later mice were o.p. treated with *E. coli*[OVA]. OTII T cell activation was determined on day 3 (unpaired *t* test). (**C** and **D**) Lung Mks present antigen in the context of MHC II in vitro. WT and MHC II^{–/–} lung Mks were incubated with OTII T cells and Ova/LPS. On day 3 T cell activation was determined by flow cytometry (unpaired *t* test). (**C**) WT lung Mks induced more T cell activation than did MHC II^{–/–} lung Mks and had (**D**) more IL-2 production on day 8. (**E**) Lung Mks present antigen in the context of MHC II in vivo. WT and Mk-specific MHC II^{–/–} mice were given OTII T cells and *E. coli*[OVA] via the o.p. route. On day 3, OTII T cell activation was determined. WT mice had more CD25-positive OTII cells and OTII T cell proliferation compared with Mk-MHC II^{–/–} mice (upaired *t* test). *P = 0.01 to 0.05, **P = 0.001 to 0.01, ***P = 0.0001 to 0.001, ****P < 0.0001.

barcoded, full-length cDNAs from polyadenylated mRNAs. After incubation, GEMs were broken and the pooled post–GEM-RT reaction mixtures were recovered and cDNA was purified with silane magnetic beads (DynaBeads MyOne Silane Beads, PN37002D, Thermo Fisher Scientific). The entire purified post–GEM-RT product was amplified by PCR. This amplification reaction generated sufficient material to construct a 3′ gene expression library. For the 3′ gene expression library, enzymatic fragmentation and size selection was used to optimize the cDNA amplicon size and indexed sequencing libraries were constructed by end repair, A-tailing, adaptor ligation, and PCR. Final libraries contained the P5 and P7 priming sites used in Illumina bridge amplification. Paired-end reads were generated for each sample using Illumina's NextSeq 550 v2. All original scRNA-seq data were deposited in the NCBI's Gene Expression Omnibus database (GEO GSE158358).

scRNA-seq analysis. Raw sequencing was processed and aligned to the *Mus musculus* genome assembly (mm10) using Cell Ranger software (v3, 10× Genomics). Subsequent quality control and secondary analysis steps were carried out using Seurat and cells with high mitochondria content (10% of total reads) were removed. Cells with very high RNA or gene content (doublets) were also excluded from downstream analysis. Technical variations such as sequencing depth, proportion of mitochondrial transcripts, and differences in cell cycle states (dividing versus nondividing) were regressed out during data normalization and scaling. For each sample, cells with similar transcriptomic profiles were grouped into specific clusters by a shared nearest neighbor (SNN) modularity optimization-based clustering algorithm. We assigned cell type identities to clusters of interest based on canonical markers.

Samples from all 3 captures (1 from BM, 2 from lungs) were integrated to investigate shared cell states across multiple data sets. Differentially expressed genes for identity classes were identified using Wilcoxon's rank sum test (Seurat FindMarkers default). Markers that are specific to each identity were then submitted to enrichR (34, 35) for gene ontology analysis.

Lung intravital imaging. Lung imaging was done after o.p. challenge with LPS and intratracheal dosing with DQ-Ova. Mice were Pf4-Cre Rosa26-LSL-tdTomato. Evans blue dye was used as a blood plasma label. Imaging started approximately 30 minutes after DQ-OVA delivery and continued for approximately 80 minutes, with each time frame taking around 95 seconds to cycle. Lung imaging used the setup procedure 2-photon microscopy techniques, and image analyses are previously described (2).

Immunohistochemistry. Lungs were fixed in 60% methanol/10% acetic acid/30% H_2O solution and 5-μm unstained sections produced by standard methodology. Slides were stained with anti-CD42c (Emfret Analytics, M050-0) at a dilution of 1:500 and were counterstained after secondary staining with a mouse anti-rat antibody. Macaque lungs were stained with anti-CD41 (Abcam, ab63983; DAB brown chromagen) at a dilution of 1:50 on the Leica Bond RX autostaining machine.

Blood collection, complete blood counts, platelet activation, and plasma isolation. Complete blood counts (CBCs) were performed using an Abaxis VetScan HM5 on mouse blood collected in EDTA tubes (VWR, 95057-293) from a retro-orbital bleed. Plasma was isolated from blood spun at 800*g* for 10 minutes. Plasma not used immediately was stored at –20°C. Platelets were activated as previously described (17).

ELISA. ELISAs were performed following the manufacturers' instructions. ELISAs included OVAL High-Sensitivity ELISA Kit (chicken) (Aviva Systems Biology, OKCD01353), Mouse TNF-α DuoSet ELISA (Thermo Fisher Scientific, DY41005), Mouse IL-6 DuoSet ELISA (Thermo Fisher Scientific, DY40605), Mouse IL-4 DuoSet ELISA (Thermo Fisher Scientific, DY40405), Mouse IL-2 DuoSet ELISA (Thermo Fisher Scientific, DY40205), Mouse IL-10 Quantikine ELISA Kit (Thermo Fisher Scientific, M1000B), and Mouse IFN-γ DuoSet ELISA (Thermo Fisher Scientific, DY485-05). The Proteome Profiler Mouse Cytokine Array Kit, Panel A (Thermo Fisher Scientific, ARY006) was used to compare BM and Mk_L cytokine expression. The methods used for the cytokine array were provided by the manufacturer. LPS (Sigma-Aldrich, L6529-1mg) was used as a stimulus in many of the Mk activation experiments.

Oropharyngeal treatment. Mice were anesthetized with isoflurane and suspended using dental floss to allow oral access. The tongue was gently encouraged out of the mouth and held in place with a pipette tip to ensure the mouse was unable to swallow. Fifty microliters of control solution or treatment was delivered into the trachea via a standard lab pipette (20–200 μL). The mouse was held in position until its breathing returned to normal.

Staining for discrimination of vascular versus tissue Mks. Methods from Anderson et al. were followed for these experiments (29). Mice were injected with anti-CD41 BV421(MWReg30, BioLegend) i.v. and then sacrificed after 3 minutes. The organs and blood were then stained ex vivo with anti-CD41 BV786 (MWReg30, BD Biosciences), allowing the discrimination of tissue and vascular Mks.

In vitro platelet production and thrombin stimulation. Using methods outlined by others (36), Mk medium that consisted of STEM-Span-ACF (STEMCELL Technologies, 09855), TPO (25 ng/mL) (Biolegend, 593304), SCF (25 ng/mL) (STEMCELL Technologies, 78064.1), IL-6 (10 ng/mL) (Biolegend, 575702), IL-9 (10 ng/mL) (Thermo Fisher Scientific, 409ML010), and heparin (5 U/mL) (Sigma-Aldrich, H3393-100KU) was utilized. Cells were plated in 35-mm glass-bottom dishes (Mat-tek). Y-27632 (STEMCELL Technologies, 72302) was as added for the first 3 days of culture and cells were incubated in 7% CO_2 at 39°C. Once platelets were observed in culture, they were collected and analyzed for CD41a/CD61 expression. Platelet rafts and Mks were imaged using differential interference contrast. Images were obtained using an Olympus IX81 inverted epifluorescence microscope outfitted with a 60× (NA 1.45) objective and Slidebook software. A motorized stage enabled live searching of platelet rafts and Mks. At least 10 fields were imaged for both lung and BM samples and the imaging experiment was repeated 4 times. Mks or platelets were isolated from culture and fresh mouse platelets were isolated as a positive control for thrombin activation. Cells were stimulated with 1 U/mL thrombin for 10 minutes and then stained with anti-CD62P antibody (Thermo Fisher Scientific, BDB553744) for 10 minutes in the dark.

Mk-lineage depletion and IL-33 depletion experiments. Mice were given 2 μg/g of anti-CD42b or the appropriate IgG control during the first day of the experiment. CBCs were obtained at 1.5 and 24 hours and lungs and BM were obtained at 24 hours to show that the lung Mks were specifically affected by the anti-CD42b (Supplemental Figures 12 and 13). On the following day the mice were given ST2-Fc (5 μg/mouse) (R&D Systems). On day 4 the mice were sacrificed. For the IL-33 depletion experiments, pups were given either ST2-Fc or

IgG (200 ng/pup) subcutaneous injections within hours of birth and again on day 4. On day 7 the pups were sacrificed with 10 minutes of CO_2 and then decapitation. After sacrificing mice for each experiment flow cytometry was used for data analysis.

BM transfer experiment. To determine whether the lung environment underlies one of the mechanisms accounting for the differences in the BM and lung Mks we wanted to see if BM Mks transferred into the lung would have an altered phenotype. BM Mks were isolated from naive WT mice and were stained with CellTrace Violet (Thermo Fischer Scientific, C34557) using the instructions from the manufacturer. Three million cells were transferred to naive WT mice via the o.p. route with either PBS or GFP *E. coli*. The mice were sacrificed 2 days later for flow cytometry.

E. coli culture and CFU count. Mice were given either *E. coli*[GFP+] (ATCC, 25922GFP) or *E. coli*[GFP+] expressing full-length Ova via o.p. administration. The Ova plasmid was obtained from AddGene (catalog 25099). Mice were given $5 × 10^7$ GFP *E. coli*. Mouse weight was monitored daily.

CFU was determined using a plate count protocol. Frozen bacterial stocks were taken from the –80°C freezer, after which a 100 μL tip was passed 3 times through the bacterial stock and then the whole tip was added to a flask with LB Broth (Thermo Fisher Scientific, BP1427-500) and 100 mg/mL of ampicillin (Thermo Fisher Scientific, BP1760-5). The cells were shaken at 37°C and 200 rpm for 19 hours. Dilutions of the bacteria were plated on LB nutrient agar plates and incubated overnight. At the end of the incubation time the plates that had fewer than 30 colonies or more than 300 colonies were discarded due to concerns about accuracy. Plates with colonies between those numbers were counted and the following equation was used to determine CFU/mL: (number of colonies [CFUs])/(dilution × amount plated) = number of bacteria/mL.

PhrodoGreen experiments. Mks were isolated from the lung and the BM and RAW 264.7 cells (ATCC, TIB-71) were used as a positive control. After the Mks were isolated the Mks and the RAW cells were allowed to rest in culture media at a pH of 7.4 at 37°C at 5% CO_2 for 1 hour. Negative controls were placed in ice for 30 minutes, while the other cells remained in the incubator. PhrodoGreen (Thermo Fisher Scientific, P35366)

particles were sonicated in a water bath for 5 minutes, transferred to wells, incubated 2 hours, cells fixed, and flow cytometry performed.

Data analysis. ELISAs were quantified using the BMG Fluostar OPTIMA and MyAssays. Flow cytometers were the Accuri C6 and BD LSR II. All flow cytometry samples were analyzed by FlowJo version 10.0.7 or version 8.7. ImageStream data were analyzed using IDEAS (Amnis).

Statistics. Statistical analyses were performed using GraphPad Prism version 7. *P* values less than 0.05 were considered significant: *P = 0.01 to 0.05, **P = 0.001 to 0.01, ***P = 0.0001 to 0.001, and ****P < 0.0001. All data are shown as mean ± SEM. All statistical tests corrected for multiple comparisons when there were more than 2 groups in an experiment.

Study approval. All experiments were performed using protocols approved by the University of Rochester Medical Center Institutional Animal Care and Use Committee (IACUC).

Author contributions

CNM, DNP, MRL, SNG, KEM, and JP designed this study. CNM, DNP, KEM, and JP contributed to drafting of the manuscript. DNP, CNM, ZTH, SKT, SKBN, SJC, ERP, JS, JV, FM, LTS, AA, ACL, SMGM, CL, KAMP, and KEM performed experiments and analyzed data. NPTH performed scRNA-seq analysis.

Acknowledgments

Address correspondence to: Craig Morrell, Aab Cardiovascular Research Institute, University of Rochester School of Medicine, Box CVRI, 601 Elmwood Ave, Rochester, New York 14642, USA. Phone: 585.276.7693; Email: Craig_Morrell@urmc.rochester.edu.

1. Morrell CN, Pariser DN, Hilt ZT, Vega Ocasio D. The platelet Napoleon complex — small cells, but big immune regulatory functions. *Annu Rev Immunol*. 2019;37:125–144.

2. Lefrançais E, et al. The lung is a site of platelet biogenesis and a reservoir for haematopoietic progenitors. *Nature*. 2017;544(7648):105–109.

3. Megakaryocytes in the lungs. *Br Med J*. 1966;1(5500):1377–1378.

4. Aabo K, Hansen KB. Megakaryocytes in pulmonary blood vessels. I. Incidence at autopsy, clinicopathological relations especially to disseminated intravascular coagulation. *Acta Pathol Microbiol Scand A*. 1978;86(4):285–291.

5. Sharnoff JG, Kim ES. Pulmonary megakaryocyte studies in rabbits. *AMA Arch Pathol*. 1958;66(3):340–343.

6. Aschoff L. Ueber capilläre Embolie von riesenkernhaltigen Zellen. *Arch Pathol Anat Phys*. 1893;134:11–14.

7. Gawaz M, Langer H, May AE. Platelets in inflammation and atherogenesis. *J Clin Invest*.

2005;115(12):3378–3384.

8. Massberg S, et al. Platelets secrete stromal cell-derived factor 1alpha and recruit bone marrow-derived progenitor cells to arterial thrombi in vivo. *J Exp Med*. 2006;203(5):1221–1233.

9. Gawaz M. Role of platelets in coronary thrombosis and reperfusion of ischemic myocardium. *Cardiovasc Res*. 2004;61(3):498–511.

10. Langer H, et al. Adherent platelets recruit and induce differentiation of murine embryonic endothelial progenitor cells to mature endothelial cells in vitro. *Circ Res*. 2006;98(2):e2–10.

11. Huo Y, et al. Circulating activated platelets exacerbate atherosclerosis in mice deficient in apolipoprotein E. *Nat Med*. 2003;9(1):61–67.

12. von Hundelshausen P, et al. RANTES deposition by platelets triggers monocyte arrest on inflamed and atherosclerotic endothelium. *Circulation*. 2001;103(13):1772–1777.

13. Boilard E, et al. Influenza virus H1N1 activates platelets through FcγRIIA signaling and thrombin generation. *Blood*. 2014;123(18):2854–2863.

14. Stifter SA, et al. Functional interplay between type I and II Interferons is essential to limit influenza A virus-induced tissue inflammation. *PLoS Pathog*. 2016;12(1):e1005378.

15. Buyukyilmaz G, Soyer OU, Buyuktiryaki B, Alioglu B, Dallar Y. Platelet aggregation, secretion, and coagulation changes in children with asthma. *Blood Coagul Fibrinolysis*. 2014;25(7):738–744.

16. Srivastava K, et al. Platelet factor 4 mediates inflammation in experimental cerebral malaria. *Cell Host Microbe*. 2008;4(2):179–187.

17. Hilt ZT, et al. Platelet-derived β2M regulates monocyte inflammatory responses. *JCI Insight*. 2019;4(5):e122943.

18. Rondina MT, et al. In vivo platelet activation in critically ill patients with primary 2009 influenza A(H1N1). *Chest*. 2012;141(6):1490–1495.

19. Aggrey AA, Srivastava K, Ture S, Field DJ, Morrell CN. Platelet induction of the acute-phase response is protective in murine experimental cerebral malaria. *J Immunol*.

2013;190(9):4685–4691.

20. Shi G, et al. Platelet factor 4 limits Th17 differentiation and cardiac allograft rejection. *J Clin Invest*. 2014;124(2):543–552.

21. Chapman LM, et al. Platelets present antigen in the context of MHC class I. *J Immunol*. 2012;189(2):916–923.

22. Zufferey A, et al. Mature murine megakaryocytes present antigen-MHC class I molecules to T cells and transfer them to platelets. *Blood Adv*. 2017;1(20):1773–1785.

23. Sharma GK, Talbot IC. Pulmonary megakaryocytes: "missing link" between cardiovascular and respiratory disease? *J Clin Pathol*. 1986;39(9):969–976.

24. McIntyre BA, Kushwah R, Mechael R, Shapovalova Z, Alev C, Bhatia M. Innate immune response of human pluripotent stem cell-derived airway epithelium. *Innate Immun*. 2015;21(5):504–511.

25. de Kleer IM, et al. Perinatal activation of the interleukin-33 pathway promotes type 2 immunity in the developing lung. *Immunity*. 2016;45(6):1285–1298.

26. Kemter AM, Nagler CR. Influences on allergic mechanisms through gut, lung, and skin microbiome exposures. *J Clin Invest*. 2019;129(4):1483–1492.

27. Tjota MY, et al. IL-33-dependent induction of allergic lung inflammation by FcγRIII signaling. *J Clin Invest*. 2013;123(5):2287–2297.

28. Gurney AL, Carver-Moore K, de Sauvage FJ, Moore MW. Thrombocytopenia in c-mpl-deficient mice. *Science*. 1994;265(5177):1445–1447.

29. Anderson KG, et al. Intravascular staining for discrimination of vascular and tissue leukocytes. *Nat Protoc*. 2014;9(1):209–222.

30. Potts KS, et al. Membrane budding is a major mechanism of in vivo platelet biogenesis. *J Exp Med*. 2020;217(9):e20191206.

31. Rate A, Upham JW, Bosco A, McKenna KL, Holt PG. Airway epithelial cells regulate the functional phenotype of locally differentiating dendritic cells: implications for the pathogenesis of infectious and allergic airway disease. *J Immunol*. 2009;182(1):72–83.

32. Brill R, Halpern MM. The frequency of megakaryocytes in autopsy sections. *Blood*. 1948;3(3):286–291.

33. Howell WH, Donahue DD. The production of blood platelets in the lungs. *J Exp Med*. 1937;65(2):177–203.

34. Stuart T, et al. Comprehensive integration of single-cell data. *Cell*. 2019;177(7):1888–1902.e21.

35. Butler A, Hoffman P, Smibert P, Papalexi E, Satija